Cell

Oncogene-Induced Senescence Relayed by an Interleukin-Dependent Inflammatory Network

Thomas Kuilman,[1] Chrysiis Michaloglou,[1,4] Liesbeth C.W. Vredeveld,[1,4] Sirith Douma,[1] Remco van Doorn,[1,5] Christophe J. Desmet,[1] Lucien A. Aarden,[2,4] Wolter J. Mooi,[3,4] and Daniel S. Peeper[1,*]
[1]Division of Molecular Genetics, The Netherlands Cancer Institute, 1066 CX Amsterdam, The Netherlands
[2]Sanquin-AMC Landsteiner Laboratory, 1066 CX Amsterdam, The Netherlands
[3]Department of Pathology, VU University Medical Center, 1081 HV Amsterdam, The Netherlands
[4]These authors contributed equally to this work
[5]Present address: Department of Dermatology, Leiden University Medical Center, 2300 RC Leiden, The Netherlands
*Correspondence: d.peeper@nki.nl
DOI 10.1016/j.cell.2008.03.039

SUMMARY

Oncogene-induced cellular senescence (OIS) is emerging as a potent cancer-protective response to oncogenic events, serving to eliminate early neoplastic cells from the proliferative pool. Using combined genetic and bioinformatic analysis, we find that OIS is linked specifically to the activation of an inflammatory transcriptome. Induced genes included the pleiotropic cytokine interleukin-6 (IL-6), which upon secretion by senescent cells acted mitogenically in a paracrine fashion. Unexpectedly, IL-6 was also required for the execution of OIS, but in a cell-autonomous mode. Its depletion caused the inflammatory network to collapse and abolished senescence entry and maintenance. Furthermore, we demonstrate that the transcription factor C/EBPβ cooperates with IL-6 to amplify the activation of the inflammatory network, including IL-8. In human colon adenomas, IL-8 specifically colocalized with arrested, $p16^{INK4A}$-positive epithelium. We propose a model in which the context-dependent cytostatic and promitogenic functions of specific interleukins contribute to connect senescence with an inflammatory phenotype and cancer.

INTRODUCTION

The ability of multicellular organisms to renew and regenerate tissues contributes to longevity. However, this capacity comes at a cost because tissue renewal sets the stage for unscheduled proliferation upon the acquirement of oncogenic lesions (Finkel et al., 2007). In isolation, such (epi)genetic lesions generally do not suffice to bring about full malignancy, although small neoplastic cell groups may result (Mooi and Peeper, 2006). Several mechanisms including apoptosis and lack of vessel formation account for their failure to continue expanding and undergo full malignant transformation (Lowe et al., 2004; Sherr, 2004). As is evident from the (virtual) absence of mitotic figures in many longstanding benign tumors, proliferative arrest, too, represents an effective mechanism suppressing continued outgrowth and the associated risk of transformation to overt cancer.

The cell-cycle arrest observed in nongrowing benign lesions like melanocytic nevi shares a number of key characteristics with cellular senescence. Indeed, several lines of evidence have recently implicated oncogene-induced cellular senescence (OIS), which is induced prematurely (that is, before telomeric shortening can account for it [Shay and Wright, 2005]), as a vital cause of arrest of benign neoplasms. It can be triggered by activated oncoproteins like $BRAF^{E600}$ or RAS^{V12} or by the loss of tumor suppressor proteins, like PTEN or NF1 (Chen et al., 2005; Michaloglou et al., 2005; Courtois-Cox et al., 2006), and occurs in a variety of cell types (Lloyd et al., 1997; Nicke et al., 2005; Denoyelle et al., 2006). OIS is often accompanied by the upregulation of the CDK inhibitors $p15^{INK4B}$, $p16^{INK4A}$, and $p21^{CIP1}$, as well as by an increase in senescence-associated β-galactosidase (SA-β-Gal) activity (Dimri et al., 1995; Campisi, 2005). Although largely irreversible, upon acute inactivation of *Rb* or *p53* genes senescence can be reversed (Beausejour et al., 2003; Dirac and Bernards, 2003; Sage et al., 2003). A further hallmark is the formation of senescence-associated heterochromatic foci (SAHF), subnuclear structures containing heterochromatin proteins that contribute to senescence by repressing the promoters of proliferation-associated genes (Narita et al., 2003; Adams, 2007). OIS has been correlated also with DNA replication stress and hyperreplication (Bartkova et al., 2006; Di Micco et al., 2006; Mallette et al., 2007).

Compelling evidence supporting OIS as a physiologically relevant mechanism limiting tumorigenesis is rapidly emerging. Senescence markers have been identified in various in vivo lesions, including human melanocytic nevi (Michaloglou et al., 2005; Gray-Schopfer et al., 2006), murine lung adenomas (Dankort et al., 2007), human dermal neurofibromas (Courtois-Cox et al., 2006), human and murine prostatic adenomas (Chen et al., 2005), murine pancreatic intraductal neoplasias (Collado et al., 2005), murine lymphomas (Braig et al., 2005) and early murine melanomas (Ha et al., 2007).

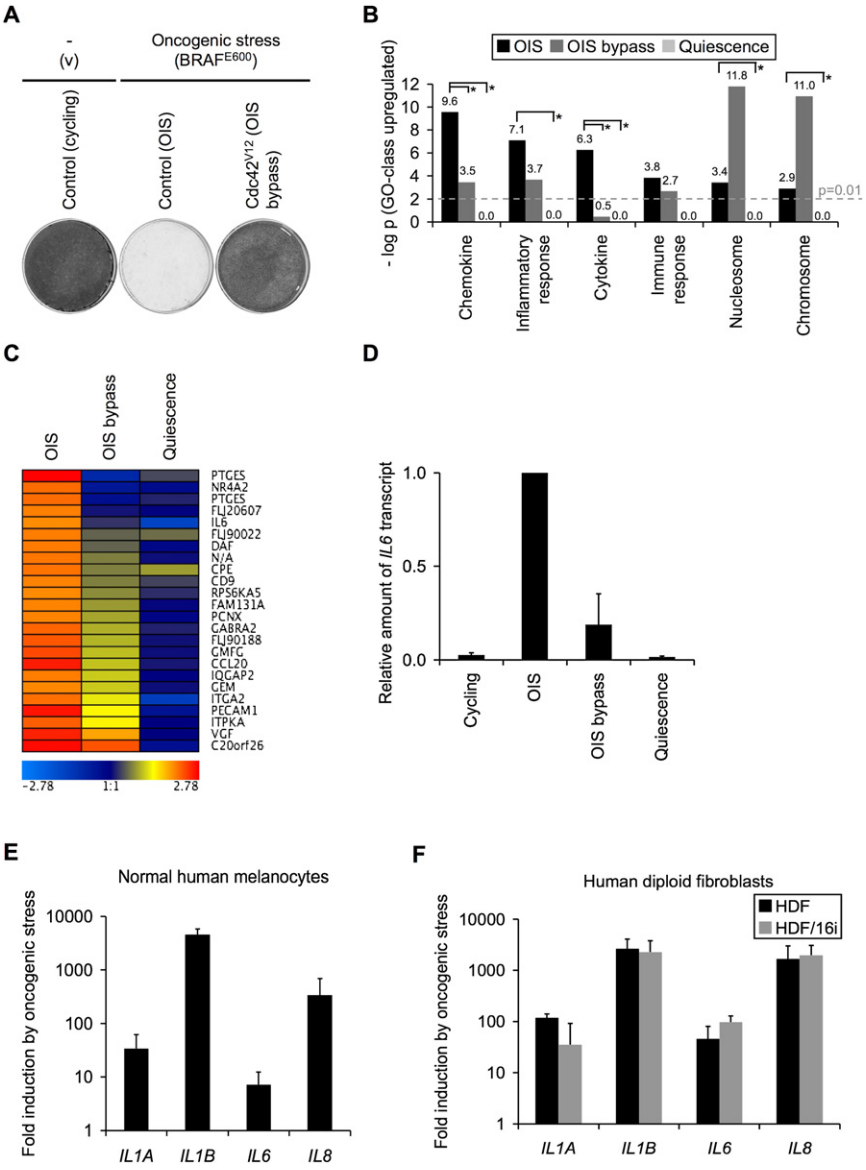

Figure 1. OIS Is Associated with Activation of an Inflammatory Transcriptome Including IL-6 Induction

(A) Cycling Tig3(et) HDF were retrovirally transduced as indicated, used in a cell proliferation assay, and fixed and stained 11 days after infection.

(B–D) Tig3(et) cells undergoing OIS (upon transduction with $BRAF^{E600}$-encoding retrovirus) or bypassing OIS (upon infection with both $Cdc42^{V12}$- and $BRAF^{E600}$-encoding retroviruses) were subjected to gene expression microarray analysis. Quiescent cells (upon 48 hr serum starvation) were included as controls. Exponentially cycling cells served as a common reference.

(B) Gene Ontology (GO) analysis was applied, and 6 of 14 significantly ($p < 0.01$) upregulated classes are represented in the chart (the full panel is represented in Figure S1). Significant ($p < 0.01$) differences in regulation of GO classes between data sets are marked (*).

(C) Heat map of ^{2}log-ratio (M) values of genes that are significantly upregulated in OIS ($M > 2$ and $p < 0.001$) but not in OIS bypass or quiescence ($M < 1$ or $p > 0.001$). These filters were applied on the complete gene expression data set, and genes were sorted according to M values in OIS bypass.

(D) Relative *IL6* transcript levels in HDF as indicated were determined by qRT-PCR. Levels are represented relative to those found in cells undergoing OIS, as mean + SD.

(E) Primary human melanocytes were lentivirally transduced with $BRAF^{E600}$, and the expression levels of several interleukin transcripts were determined by qRT-PCR. Levels are represented relative to those found in cycling cells, as mean + SD.

(F) As in (E), but in Tig3(et) without (black bars) or with (gray bars) *sh*-$p16^{INK4A}$. Data are represented as mean + SD.

Because a picture emerges of a substantial role for OIS in the prevention of cancer, several attempts are being made to further resolve its mechanism. For example, function-based genome-wide screens have unraveled unanticipated tumorigenic mechanisms (Peeper et al., 2002; Berns et al., 2004; Rowland et al., 2005). Despite such recent progress, we are only beginning to unveil the molecular mechanism of OIS and to identify the key players involved. By using a combination of gene expression profiling and RNA interference, we set out to uncover previously unidentified pathways that relay OIS.

RESULTS

OIS Is Associated with Activation of an Inflammatory Transcriptome

To conduct an unbiased search for novel pathways mediating OIS, we studied cellular senescence resulting from oncogenic signaling by $BRAF^{E600}$. This common cancer-derived mutant protein kinase can contribute to oncogenic transformation if placed in the context of additional genetic lesions (Davies et al., 2002; Garnett and Marais, 2004). However, when introduced into human diploid fibroblasts (HDF) in the absence of cooperating lesions, $BRAF^{E600}$ induces a robust cell-cycle arrest. This is associated with many hallmarks of senescence, including induction of $p16^{INK4A}$ (Michaloglou et al., 2005). To identify genes that are transcriptionally upregulated during OIS and in turn decline during OIS bypass, we performed genome-wide expression microarray analysis (Figure 1A; ArrayExpress accession number E-NCMF-12).

Unbiased gene ontology (GO) analysis of the microarray data sets revealed 14 out of 1158 GO classes to be significantly upregulated during exposure to oncogenic stress ($p < 0.01$; Figure S1 and Table S1 available online). Compared to cells that had undergone senescence, cells that bypassed OIS showed a sharp and significant ($p < 0.01$) decrease in the extent of upregulation of the "cytokine" and "chemokine" GO classes (each comprising ~50 genes), whereas neither category was significantly

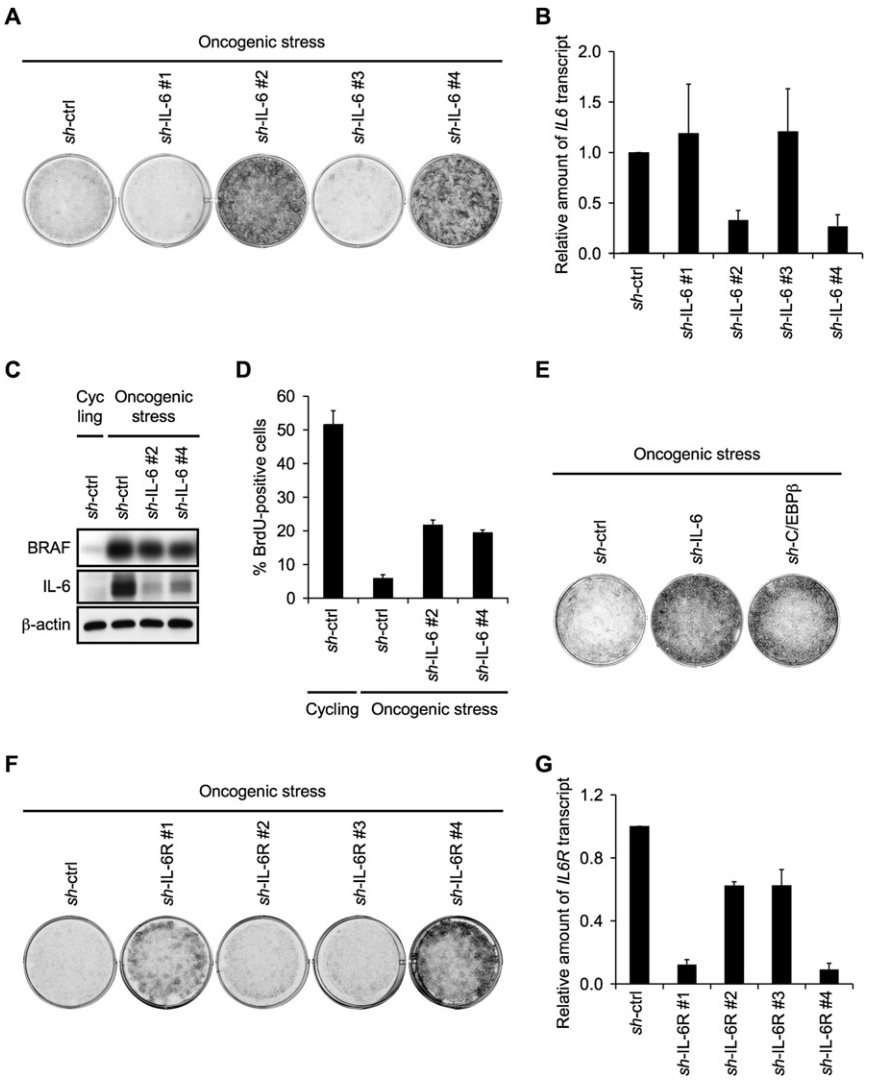

Figure 2. A Critical Role for IL-6 in Mediating OIS

(A) Cell proliferation assay of polyclonal Tig3(et)/16i HDF expressing independent, nonoverlapping shRNAs against IL-6 upon exposure to oncogenic stress (transduction with $BRAF^{E600}$-encoding retrovirus). Cells were fixed and stained 15 days after infection.

(B) Samples from (A) were analyzed for *IL6* transcript levels by qRT-PCR. Levels are represented relative to those found in control-infected cells, as mean + SD.

(C) Samples from (A) were analyzed by western blotting for protein expression as indicated. β-actin serves as loading control.

(D) BrdU incorporation of Tig3(et)/16i cells after retroviral transduction with the indicated shRNAs and labeling at 11 days after exposure to oncogenic stress ($BRAF^{E600}$ retrovirus infection). Data are represented as mean + SD.

(E) Cell proliferation assay of senescent ($BRAF^{E600}$-expressing) Tig3(et) cells plated at equal densities and subsequently transduced with lentivirus expressing *sh*-IL-6 or *sh*-C/EBPβ. Cells were fixed and stained 8 days after infection.

(F) Cell proliferation assay of polyclonal Tig3(et)/16i HDF expressing independent, nonoverlapping shRNAs against IL-6R upon exposure to oncogenic stress (transduction with $BRAF^{E600}$-encoding retrovirus). Cells were fixed and stained 15 days after infection.

(G) Samples from (F) were assessed for *IL6R* transcript levels by qRT-PCR. Levels are represented relative to those found in control-infected cells, as mean + SD.

upregulated in quiescence. These properties distinguished these GO classes from all other significantly upregulated ones (Figure 1B). Thus, OIS is specifically associated with the activation of a cytokine and chemokine response.

To deconvolute the GO classes and identify genes strongly associated with OIS, we applied the same three criteria (i.e., induction by oncogenic stress, significantly less induction during OIS bypass, and quiescence) on the raw gene expression data set. This yielded a collection of 24 genes, including interleukin-6 (IL-6; Figure 1C). Ingenuity pathway analysis (IPA) and gene set enrichment analysis (GSEA) further supported the notion that the IL-6 pathway is activated during OIS (Figure S2 and data not shown). IL-6 is a cytokine implicated in a variety of cellular functions, including immune response, proliferation, and tumorigenesis (Hirano and Kishimoto, 1989). Because IL-6 can act as a potent inducer of growth arrest and/or differentiation (Hong et al., 2007) and correlates with RAS^{V12}-induced senescence in murine embryonic fibroblasts (Mason et al., 2004), we focused our attention on this cytokine as a candidate OIS gene.

Specific Upregulation of IL-6 during OIS

We reasoned that if IL-6 mediates OIS, it should meet three criteria. First, its expression levels must mirror OIS induction and bypass. Indeed, quantitative RT-PCR (qRT-PCR) analysis, while confirming the sharp induction of *IL6* transcript levels observed by microarray analysis, revealed a significant correlation between *IL6* expression and OIS and OIS bypass (Figure 1D). Second, IL-6 induction by oncogenic stress must be independent of cellular context. RNA and protein analyses of HDF and primary human melanocytes showed that IL-6 (as well as IL-1α, IL-1β, and IL-8) was upregulated by oncogenic signaling to 1–3 orders of magnitude, irrespective of cell type (Figures 1E, 1F, and 2C). This is consistent with previous reports on expression of interleukins, including IL-6 and IL-8, being increased in senescent cells (Mason et al., 2004; Schnabl et al., 2003), and these reports also indicate that this is seen for different cell types and for oncogenes in addition to $BRAF^{E600}$. Third, the induction of IL-6 by oncogenic stress must be independent of $p16^{INK4A}$. This relates to our previous finding that although $BRAF^{E600}$ induces $p16^{INK4A}$, $BRAF^{E600}$-induced senescence in HDF occurs independently of $p16^{INK4A}$ (Michaloglou et al., 2005). This criterion was met, too, as we failed to detect a significant difference

in the levels of IL-6 upon exposure to oncogenic stress whether $p16^{INK4A}$ was present or absent (Figure 1F). Thus, IL-6 is upregulated specifically during OIS, independent of cell type and $p16^{INK4A}$ status.

A Critical Role for IL-6 in Mediating OIS

To investigate whether IL-6 is causally involved in OIS, we designed several nonoverlapping short hairpin RNAs (shRNAs) targeting IL-6. Although $p16^{INK4A}$ is not strictly required for $BRAF^{E600}$-induced senescence in HDF, it may well contribute to it, in the context of additional factors (Michaloglou et al., 2005). For that reason, we generated HDF expressing a shRNA targeting $p16^{INK4A}$ ('Tig3(et)/16i'), from which polyclonal cell lines expressing distinct IL-6 shRNAs were derived. These were transduced with $BRAF^{E600}$-encoding retrovirus, selected for proviral integration, and plated at equal densities. A cell proliferation assay showed that IL-6 depletion caused cells to efficiently bypass OIS (Figure 2A). A close correlation was observed between the extent of IL-6 knockdown and the biological effect, arguing against RNAi off-target effects (Figures 2A–2C). Importantly, the OIS bypass was not due to loss of $BRAF^{E600}$ expression. To quantify the rescue from senescence, we performed a BrdU-incorporation assay to measure the extent of DNA replication. The number of cells actively replicating DNA in the presence of oncogenic stress increased by ~4-fold upon IL-6 depletion (Figure 2D). To determine whether IL-6 is required not only for induction but also for the maintenance of OIS, we transduced senescent HDF cultures with lentivirus expressing *sh*-IL-6 and monitored the cultures for proliferative activity. IL-6 depletion led to reversal of OIS, with cells re-entering the cell cycle and resuming proliferation (Figure 2E; Figure S3; the results on C/EBPβ are discussed below). Thus, IL-6 is required for both induction and maintenance of OIS. Because this experiment was performed in normal HDF, this result shows also that the IL-6-dependency is observed whether $p16^{INK4A}$ is absent or present.

Not only IL-6 but also its cognate receptor, IL-6R/GP80, was upregulated in senescent cells, as measured by qRT-PCR (Figure S4). To determine whether in addition to IL-6 its receptor is also required for the mediation of OIS, we designed a set of shRNAs targeting IL-6R. We found that IL-6R depletion caused cells to bypass OIS, as evident by a cell proliferation assay (Figures 2F and 2G) and BrdU incorporation (Figure S5). Also in an independent HDF strain (IMR90), IL-6 and its receptor were required for OIS induction and maintenance (Figures S6A and S6B). We conclude that the IL-6/IL-6R pathway plays an essential role in mediating OIS.

IL-6 Inhibits Proliferation in the Context of Oncogenic Stress

Next, we examined whether IL-6 signaling is not only required for OIS but also sufficient to induce it by treating cell cultures with a combination of recombinant IL-6 (rIL-6) and recombinant soluble IL-6R (rsIL-6R). As a positive control, the human melanoma cell line A375, one of the few melanomas that undergoes cell-cycle arrest in response to IL-6 signaling, was used. Whereas activated IL-6 signaling caused A375 cells to cease proliferating, it failed to trigger arrest in HDF (Figure 3A). Similar results were obtained when we overexpressed *IL6* cDNA (Figures 3B and 3C; note that ectopically expressed IL-6 was expressed to much higher levels than those resulting from oncogenic signaling). In contrast, and consistent with the IL-6-induced arrest of melanoma cells (harboring the $BRAF^{E600}$ mutation), IL-6 markedly augmented the ability of cells under oncogenic stress to respond with cell-cycle arrest (Figure 3B). Thus, in the presence of oncogenic stress, IL-6 can exert an antiproliferative effect. A mechanistic explanation for this observation will be discussed in the context of experiments shown below.

IL-6 Acts in a Cell-Autonomous Fashion in OIS

Since IL-6 acts through autocrine as well as paracrine signaling, we next determined which pool of IL-6 is required in OIS. Oncogenic signaling induced both intracellular and secreted IL-6 by a factor of 10 to 30, to more than 3 ng/ml (Figure S7 and data not shown). To examine the role of the secreted IL-6 pool, we treated the cell culture medium with specific neutralizing antibodies. mAb IL-6.8 prevents the interaction between IL-6 en IL-6R, while mAb IL-6.16 blocks the interaction between IL-6-IL-6R complex and gp130 (Brakenhoff et al., 1994; Kalai et al., 1997). Preincubation of cells with IL-6.8 mAb completely abolished rIL-6-induced STAT3-phosphorylation, validating the neutralizing capacity of this antibody (Figure 3D). This was further illustrated by the observation that even with 5 ng/ml rIL-6 added to a 1:20 dilution of the IL-6.8 mAb-containing culture medium of OIS cells, the total bioavailable IL-6 was effectively neutralized (Figure 3E). Then, we performed an OIS bypass assay, with the conditions such that the ratio of inhibitory antibody over IL-6 concentration was more than 10-fold higher than in the control STAT3 neutralization experiment above. Whereas *sh*-IL-6 caused cells to bypass OIS, cells treated with either IL-6 mAb remained senescent (Figure 3F). From this, we conclude that IL-6 acts in a cell-autonomous fashion to implement OIS. As this signaling cascade requires also the IL-6R to be intact (Figure 2F), these results suggest that IL-6 acts in an autocrine manner to regulate OIS.

As a paracrine factor, secreted IL-6 contributes to tumorigenesis by promoting angiogenesis (Ancrile et al., 2007). To investigate whether IL-6 secreted by senescent cells is endowed with any promitogenic activity, we collected the medium from OIS cells and transferred it to B9 hybridoma cells, which are IL-6-dependent for proliferation. This led to a remarkable reversal of their cell-cycle arrest (Figure 3G). Depletion with IL-6 antibody completely abrogated this effect, indicating that the essential promitogenic activity secreted by the senescent cells corresponded to IL-6, which acted in a paracrine fashion. Thus, whereas OIS requires a cell-autonomous pool of IL-6 that acts in an autocrine fashion, this result shows that the same senescent cells produce an IL-6 pool that acts promitogenically in a paracrine fashion.

C/EBPβ Is a Critical Regulator of IL-6 in OIS

Having identified IL-6 as an essential regulator of OIS, we next wished to resolve the mechanism by which the oncogenic signal is relayed to IL-6. In addition to *IL6*, many of the inflammatory genes that were activated during OIS, including *IL1B* and *IL8* (Figures 1E and 1F), are regulated by the transcription factor C/EBPβ. Because the IL-6 promoter contains a perfect consensus

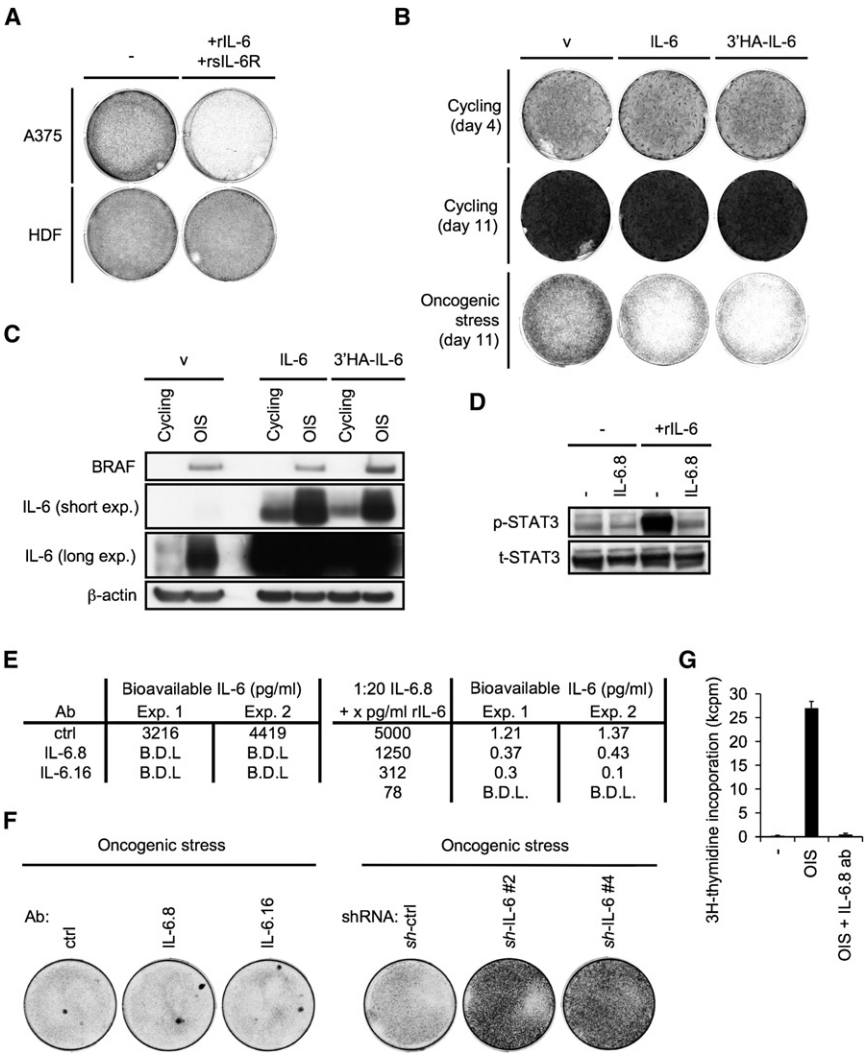

Figure 3. IL-6 Inhibits Proliferation in the Context of Oncogenic Stress and Acts in a Cell-Autonomous Fashion in OIS

(A) Cell proliferation assays of A375 human melanoma cells and Tig3(et)/16i HDF treated with recombinant IL-6 (rIL-6) and recombinant soluble IL-6R (rsIL-6R), fixed, and stained after 4 days.

(B) The proliferative potential of polyclonal Tig3(et)/16i HDF expressing IL-6 (HA-tagged or untagged, as indicated) was determined in a cell proliferation assay in the presence and absence of oncogenic stress (transduction with $BRAF^{E600}$ retrovirus).

(C) Samples from (B) were assessed by western blotting for protein expression as indicated. β-actin serves as loading control.

(D) HepG2 cells were treated with rIL-6, in the presence or absence of IL-6.8 mAb, and the expression levels of phosphorylated STAT3 (p-STAT3) and total STAT3 (t-STAT3) were determined by western blotting.

(E) Left: Quantification of the amount of bio-available IL-6 in Figure 3F employing the B9 (hybridoma growth factor) assay. Right: Same quantification after dilution of the IL-6.8 antibody and addition of different amounts ("x") of rIL-6. B.D.L., below detection limit.

(F) Left: Cell proliferation assay of oncogenically stressed ($BRAF^{E600}$-expressing) Tig3(et)/16i HDF treated with either of two neutralizing IL-6 mAbs (6.8 and 6.16) or control antibody. Right: Cells that bypassed OIS owing to shRNA-mediated IL-6 depletion serve as controls.

(G) ^{3}H-thymidine-incorporation proliferation assay in B9 hybridoma cells on medium collected from OIS cells in the absence or presence of the IL-6.8 antibody, compared to no treatment. Data are represented as mean + SD.

binding site for this transcription factor (Figure 4A), we asked whether C/EBPβ is critically involved in the regulation of these interleukins, and in OIS. First, we determined whether it is activated as a function of oncogenic stress. Indeed, several C/EBPβ isoforms (including LIP and LAP, which are generated by differential start site usage and proteolytic cleavage [Ramji and Foka, 2002]), were upregulated during OIS (Figure 4B). This was accompanied by an almost 10-fold elevation of *CEBPB* mRNA, as determined by qRT-PCR (see below), suggesting that this reflects the primary mode of activation in this setting. Consistently, C/EBPβ DNA-binding capacity was increased (Figure 4C, Figure S8). To confirm this interaction in living cells, chromatin immune precipitation (ChIP) was performed. As assayed with two independent C/EBPβ antibodies, we observed that C/EBPβ bound to the *IL6* promoter in vivo upon exposure of cells to oncogenic stress (Figure 4D). Depletion of C/EBPβ strongly diminished this binding, further validating the specificity of the signal. Thus, during OIS, C/EBPβ is recruited to the *IL6* promoter in vivo.

These results raised the possibility that C/EBPβ has an essential role in OIS. Indeed, shRNAs that successfully targeted C/EBPβ (Figure 4E) led to continued cell proliferation in the face of oncogenic stress (Figure 4F). In an independent experiment, OIS bypass by C/EBPβ depletion was quantified by BrdU incorporation (Figure S5). Similar to IL-6, C/EBPβ was required also for maintenance of OIS (Figure 2E). The induction of IL-6 by oncogenic stress and the recruitment of C/EBPβ to the *IL6* promoter argued that C/EBPβ mediates OIS by conveying the oncogenic signal to the *IL6* promoter. This was confirmed by the steep drop in the transcript and protein levels of IL-6 upon depletion of C/EBPβ (Figures 4G and 4H). As discussed for Figure 1, oncogenic stress elicited the activation of multiple interleukins, including IL-8. Expression of this latter cytokine, which mainly functions as a chemoattractant for neutrophils at sites of inflammation, is also regulated by C/EBPβ. Therefore, we examined whether IL-8, too, is expressed during OIS as a function of C/EBPβ. Indeed, C/EBPβ depletion caused *IL8* mRNA to decline to background levels (Figure 4G). These findings extend a previous observation that C/EBPβ is involved in RAS^{V12}-induced senescence in murine cells (Sebastian et al., 2005). Although not precluding an involvement of other signaling pathways, these results demonstrate that C/EBPβ is a critical

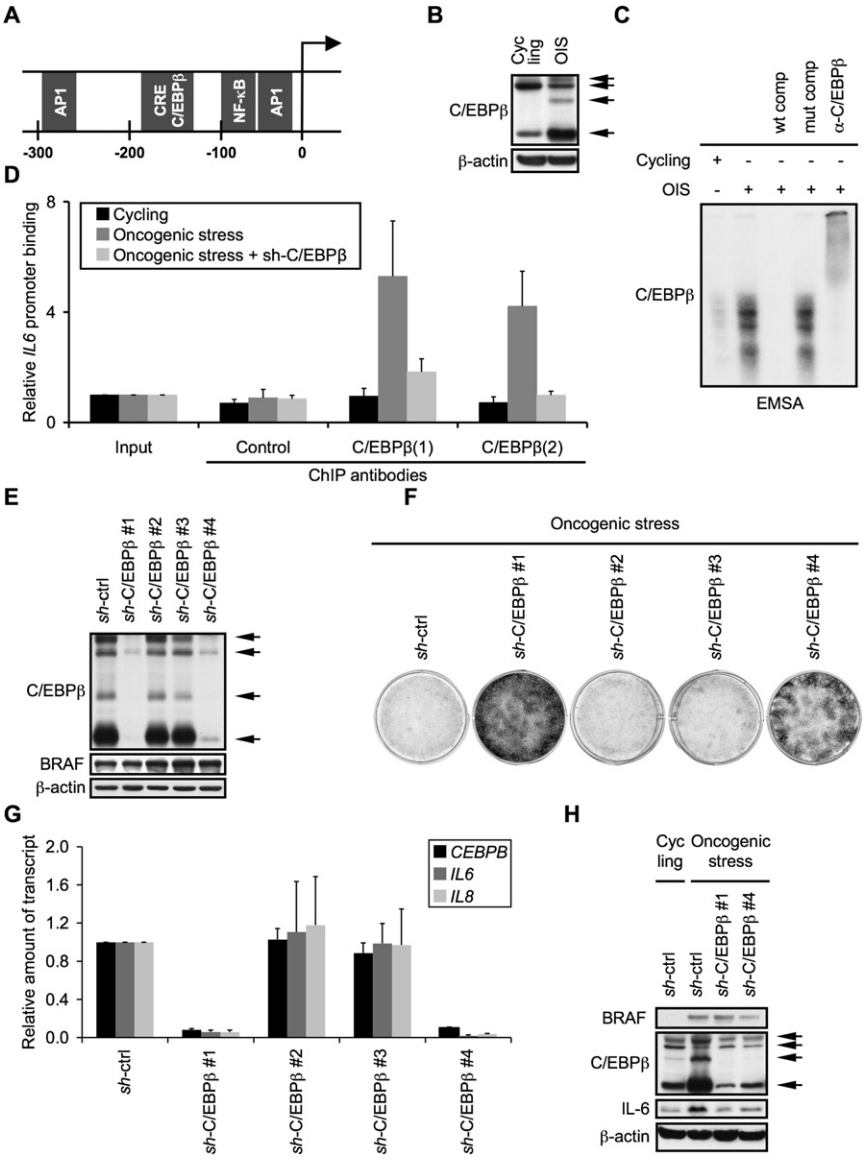

Figure 4. C/EBPβ Is a Critical Regulator of IL-6 in OIS

(A) Schematic representation of several transcription factor binding sites in the *IL6* promoter (not all sites are indicated).

(B) C/EBPβ protein expression of cycling and OIS Tig3(et)/16i HDF, as determined by western blotting. β-actin serves as loading control.

(C) Electrophoretic mobility shift assay (EMSA) on nuclear lysates from cycling and OIS cells with the C/EBPβ-binding site of the *IL6* promoter as a radiolabeled probe. Unlabeled wild-type and mutant probe competitions (250-fold excess) and antibody treatment were used to determine the specificity of the assay.

(D) Chromatin immunoprecipitation (ChIP) determining the in vivo binding of C/EBPβ to the *IL6* promoter upon exposure to oncogenic stress ($BRAF^{E600}$ retroviral infection). To determine specificity, we used two independent C/EBPβ antibodies (1, Cell Signaling, and 2, GeneTex), along with a control (anti-TrkB) antibody, on chromatin isolated from cycling and OIS cells. OIS cells expressing *sh*-C/EBPβ were included as an extra control for the specificity of C/EBPβ antibodies. Relative *IL6* promoter binding was plotted as mean + SD.

(E–H) Polyclonal Tig3(et)/16i cell lines expressing independent, nonoverlapping shRNAs for C/EBPβ were subjected to oncogenic stress (infection with $BRAF^{E600}$ retrovirus).

(E) C/EBPβ and BRAF protein levels, as determined by western blotting. β-actin serves as loading control.

(F) Cell proliferation assay of polyclonal Tig3(et)/16i HDF expressing independent shRNAs against C/EBPβ. Cells were fixed and stained 15 days after infection.

(G) Samples from (F) were assessed for *CEBPB*, *IL6*, and *IL8* transcript levels by qRT-PCR. Levels are represented relative to those found in control-infected cells, as mean + SD.

(H) BRAF, C/EBPβ, and IL-6 protein levels, as determined by western blotting. β-actin serves as loading control.

mediator in an interleukin pathway leading to OIS of human fibroblasts.

IL-6 Depletion Correlates with Reduced Formation of SAHF and Deregulation of $p15^{INK4B}$ Expression

Senescent cells often accumulate SAHF. These subnuclear structures contain heterochromatin proteins and are produced upon cellular exposure to stress. To examine whether IL-6-dependent OIS correlates with SAHF formation, we performed fluorescence stainings for K9M-H3 and DNA. In parallel, we performed a cell proliferation assay to monitor the induction and bypass of OIS. As expected, cells exposed to oncogenic stress accumulated SAHF, along with K9M-H3 modification (Figure 5A). In contrast, OIS bypass upon IL-6 depletion was associated with a marked decline in the number of cells containing SAHF. Consistent with its role in OIS, similar observations were made for C/EBPβ. These results reveal a correlation between IL-6 and SAHF formation. Although further study will be required to determine their exact relationship, a role for IL-6 in the regulation of chromatin is not unprecedented (Hodge et al., 2001).

To begin probing for connections between interleukin signaling and the cell-cycle machinery, we determined the expression of several cell-cycle genes, including all four *INK4* genes (encoding $p15^{INK4B}$, $p16^{INK4A}$, $p18^{INK4C}$, and $p19^{INK4D}$). Whereas $p16^{INK4A}$ was moderately induced by oncogenic stress, $p15^{INK4B}$ was upregulated more than 20-fold (Figures 5B and 5C). Unexpectedly, the induction of $p15^{INK4B}$ was markedly suppressed by depletion of IL-6 (Figures 5D and 5E). Adding to the significance of this finding, depletion of C/EBPβ also diminished the induction of $p15^{INK4B}$ by oncogenic stress (Figures 5F and 5G). This was specific for $p15^{INK4B}$ and not a general effect on the cell-cycle machinery, as it was not observed for $p16^{INK4A}$. Because C/EBPβ binds to the *CDKN2B* promoter in response to cytokine stimulation (Gomis et al., 2006), their communication

is likely to be direct. Conversely, ectopic expression of C/EBPβ was sufficient to bring about cell-cycle arrest (Figures 5H and 5I), extending previous data in murine cells (Sebastian et al., 2005). This was associated with a concomitant induction of $p15^{INK4B}$ and IL-6, showing that this transcription factor is also sufficient to activate the cytostatic IL-6-$p15^{INK4B}$ axis (Figures 5J and 5K). These data demonstrate that $p15^{INK4B}$ is regulated by oncogenic stress, in a significant part in a C/EBPβ-IL-6-dependent manner.

Although $p15^{INK4B}$, when expressed at high levels, induced cell-cycle arrest (data not shown), lower levels acted only weakly cytostatically (Figure S9). Whereas IL-6 was insufficient to inhibit proliferation in the absence of oncogenic stress (Figures 3A and 3B), in the context of $p15^{INK4B}$ it elicited a strong cytostatic effect (Figure S9). It thus appears that $BRAF^{E600}$ triggers activation of $p15^{INK4B}$, IL-6, and IL-6R, which act in concert to impose cell-cycle arrest.

IL-6 Is a Central Regulator of an Inflammatory Network Mediating OIS

To investigate the mechanism by which IL-6 acts as a critical mediator of OIS, we investigated its effects on the transcriptome. We performed microarray expression analysis on cells exposed to oncogenic stress, in the absence or presence of IL-6 shRNA (Figure 6A; ArrayExpress accession number E-NCMF-13). Unbiased analysis of transcriptional changes in GO classes revealed a distinct pattern for the inflammatory network. Compared to cells that had undergone OIS, cells that bypassed OIS owing to depletion of IL-6 showed a strong suppression of the inflammatory response (Figure 6B, 6C; Figure S10, and Table S2). Strikingly, this pattern was very similar to that of cells that had not been exposed to oncogenic stress at all, as well as of cells that had bypassed OIS because of the silencing of C/EBPβ. This effect was specific, as we failed to observe it for other GO classes such as "receptor" and "cytosolic $[Ca^{2+}]$ elevation." Thus, IL-6 fulfils a central role in keeping the genetic inflammatory network in an active state: Upon IL-6 depletion, the network collapses and cells bypass OIS.

To validate these results, we quantified the transcript levels for interleukins that fell into the significant outlier GO classes related to inflammation. This confirmed our microarray results and demonstrated that all of these cytokines are activated by oncogenic stress in an IL-6-dependent manner (Figure 6D). Remarkably, IL-6 depletion caused a marked decrease in the levels of C/EBPβ, too (Figure 6D). This would argue that there is a two-way communication between IL-6 and C/EBPβ, possibly a positive feedback loop, with IL-6 acting as a positively acting factor to maintain or activate the loop and C/EBPβ corresponding to the transcription factor directly regulating target genes. This predicts that C/EBPβ and IL-6 control a large set of overlapping genes within the inflammatory transcriptome, which was in fact already suggested by the heat map in Figure 6C. However, because this heat map was limited to genes that are significantly regulated, we also tested this hypothesis in an unbiased manner. Complete data sets for C/EBPβ- or IL-6-depleted cells were compared in a two-sample correlation plot. This confirmed that there is a highly significant overlap of genes regulated by each C/EBPβ and IL-6: 1084 genes were coregulated by C/EBPβ and IL-6, and only three genes were antiregulated (Figure 6E). These results argue that the mechanism by which IL-6 controls the cellular response to oncogenic signaling involves a positive feedback loop with C/EBPβ, which acts to sustain and amplify the activation of the inflammatory network.

IL-8 Plays a Role in OIS

This model raises the question whether the role of IL-6 is unique among several other interleukins being activated in response to oncogenic stress. These include IL-8, whose expression levels rise up 1000-fold in response to oncogenic signaling (Figures 1E and 1F), in a strictly IL-6-dependent manner (Figure 6D). We reasoned that the observed effect of IL-6 on IL-8 expression points to an involvement of the C/EBPβ transcription factor, for which we thus investigated a possible relationship with IL-8. ChIP analysis revealed that C/EBPβ was recruited to the *IL8* promoter in response to oncogenic stress, just like it is recruited to the *IL6* promoter (Figure 6F). Because C/EBPβ and IL-6 apparently act in a positive feedback loop, this observation further connects these interleukins during oncogenic signaling. To examine any biologically relevant role of IL-8 in this setting, we generated specific shRNAs and determined whether they interfere with OIS. Similar to what we had observed for IL-6, knockdown of IL-8 led to efficient OIS bypass (Figure 6G, Figure S11). Thus, the critical role of IL-6 in OIS is shared by IL-8, which is expressed as a function of IL-6.

IL-8 Colocalizes with $p16^{INK4A}$ in Growth-Arrested, Human Colon Adenoma Cells

To find in vivo correlates of our observations made in vitro, we analyzed the expression of IL-8 in human colon adenomas. We choose this lesion because it contains cell groups displaying two hallmarks of cellular senescence, strong $p16^{INK4A}$ immunopositivity and absence of both mitotic figures and Ki-67 positivity, as previously reported (Dai et al., 2000). These cell groups alternate with stretches of $p16^{INK4A}$-negative ones containing many Ki-67-positive cells. Of 20 adenomas tested, 19 contained areas and stretches of cells with distinct IL-8 positivity, associated with absence of Ki-67-positive nuclei, indicating proliferative arrest (Figure 7A). These arrested cell stretches stood out against adjacent areas of proliferating, IL-8-negative adenoma. In 18 out of these 19 samples, stretches of $p16^{INK4A}$ positivity largely overlapped with the nonproliferating, IL-8-positive adenoma areas. Occasionally, focal IL-8 positivity was observed also in arrested cell groups that were negative for $p16^{INK4A}$ staining (Figure S12). Compared to $p16^{INK4A}$ immunopositivity, variations in IL-8 positivity were generally more gradual, with the highest intensity observed in the areas with absent or very few Ki-67-positive nuclei. These results support a model in which interleukins contribute to OIS in vivo.

DISCUSSION

Although accumulating evidence suggests that OIS constitutes a vital protective system restricting the expansion of incipient neoplastic cells, its mechanism is not well understood. By expression profiling, we found that ~1% of all GO classes were upregulated upon exposure of cells to oncogenic signaling ($BRAF^{E600}$). However, only two classes, "cytokine" and

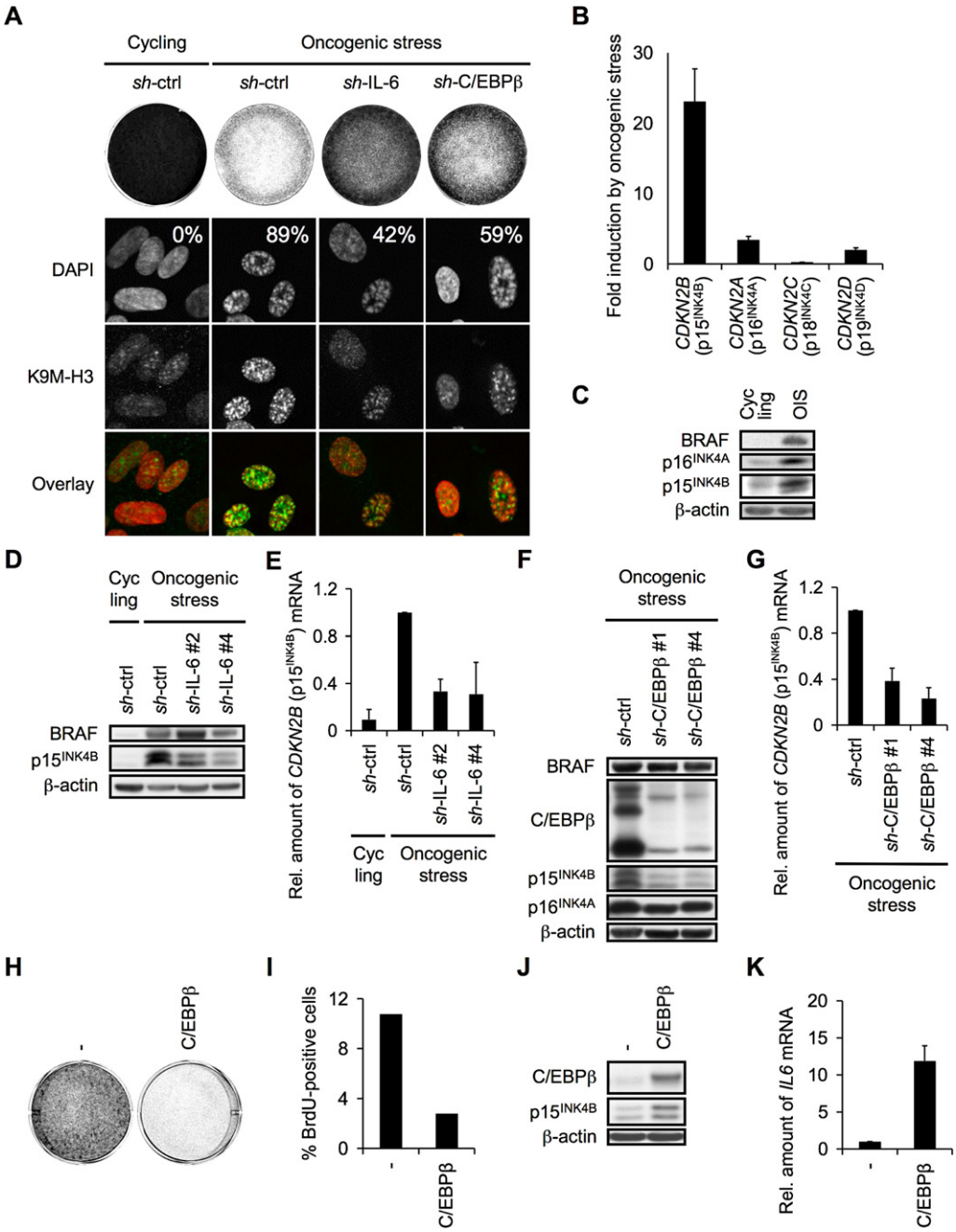

Figure 5. IL-6 Depletion Correlates with Reduced Formation of SAHF and with Deregulation of $p15^{INK4B}$ Expression

(A) Confocal microscopy images of cycling and polyclonal Tig3(et)/16i cell lines expressing *sh*-IL-6 or *sh*-C/EBPβ upon exposure to oncogenic stress ($BRAF^{E600}$ retroviral transduction). Immunofluorescence was performed for K9M-H3 (green in the overlay), and DAPI staining (red in the overlay) was used to visualize DNA. Percentages of SAHF-positive cells are indicated. In parallel, a cell proliferation assay was performed (top).

(B) Induction of *INK4*-family transcript levels in OIS Tig3(et) cells relative to cycling cells, as determined by qRT-PCR and represented as mean + SD.

(C) Samples from (B) were analyzed by western blotting for BRAF, $p15^{INK4B}$, and $p16^{INK4A}$ protein expression as indicated. β-actin serves as loading control.

(D) $p15^{INK4B}$ and BRAF protein levels as a function of IL-6 depletion, as determined by western blotting. β-actin serves as loading control.

(E) *CDKN2B* RNA levels as a function of IL-6 depletion, as determined by qRT-PCR. Data are represented as mean + SD.

(F) Determination by western blotting of protein levels as indicated, as a function of C/EBPβ depletion. β-actin serves as loading control.

(G) *CDKN2B* RNA levels as a function of C/EBPβ depletion, as determined by qRT-PCR. Data are represented as mean + SD.

(H) Cell proliferation assay for control and C/EBPβ-overexpressing IMR90(et)/16i cells. Cells were fixed and stained 10 days after infection.

(I) BrdU-incorporation of samples in (H). Cells were labeled 8 days after infection with C/EBPβ-encoding retrovirus. A representative experiment out of three independent experiments is shown.

"chemokine," in turn declined during OIS bypass. RNAi experiments revealed a causal relationship between the induction of some of these cytokines, in particular IL-6 and IL-8, and the ability of cells to undergo OIS. IL-6 is a pleiotropic cytokine that can function as an autocrine or paracrine tumorigenic factor. We show that senescent cells can act as the source of such a promitogenic IL-6 pool. We also find that in OIS, unexpectedly, IL-6 is required in a cell-autonomous manner to implement cell-cycle arrest. Because OIS apparently requires an intact IL-6R, too, our results suggest that IL-6 acts in an autocrine and cell-autonomous fashion to implement OIS. Similar results are reported in an accompanying paper by Gil and colleagues (Acosta et al., 2008), showing that CXCR2-binding chemokines expressed by senescent cells regulate growth arrest.

In response to oncogenic stress, both *IL6* and *IL8* genes were activated by the transcription factor C/EBPβ, upon its recruitment to either promoter. C/EBPβ depletion caused cells to bypass OIS effectively, which correlated with the loss of expression of both interleukins. Because, conversely, IL-6 depletion was followed by a strong decline in the levels of both C/EBPβ and IL-8, our results suggest that C/EBPβ and IL-6 constitute a positive feedback network regulating OIS. In parallel to these observations in vitro, we observed a correlation between increased IL-8 expression and $p16^{INK4A}$ immunopositivity in growth-arrested cells in human colorectal adenomas. This supports a model in which activation of the cytokine network contributes to OIS in vivo.

Oncogenic stress triggered also the induction of the CDK inhibitor $p15^{INK4B}$, which was dependent on the presence of both IL-6 and C/EBPβ. As such, this result establishes a link between OIS-activated interleukin signaling and the cell-cycle machinery. Our results suggest that IL-6 acts in concert with its receptor and $p15^{INK4B}$ to cause cell-cycle arrest in response to oncogenic stress. Although not strictly required for fibroblast OIS, it is conceivable that $p16^{INK4A}$, if induced, contributes as well. Such a model would be in line with the recent finding that in the absence of $p16^{INK4A}$, $p15^{INK4B}$ acts as a critical tumor suppressor (Krimpenfort et al., 2007).

A cytostatic role for IL-6 in specific contexts is consistent with a large body of observations (Hong et al., 2007). We consider it unlikely that the IL-6 (or IL-8) pools required for OIS (this paper), and for promoting oncogenicity (Sparmann and Bar-Sagi, 2004; Ancrile et al., 2007) or cell proliferation (this paper) are inherently different. Instead, we suggest that the genetic makeup of the IL-6 target cell, whether normal or transformed, contributes to specifying the biological response to IL-6. In keeping with this, IL-6 inhibits proliferation of early- but not advanced-stage melanoma cells (Lu and Kerbel, 1993). This duality is reminiscent of that of another cytokine, transforming growth factor β (TGF-β), which restrains the proliferation of nonmalignant cells but upon overexpression in tumor cells fosters expansion and metastasis. This parallel between IL-6 and TGF-β extends further, as defects in signaling by the latter cytokine, too, allow cells to overcome OIS, which is associated with suppression of $p15^{INK4B}$ (Tremain et al., 2000). Furthermore, two other secreted factors, PAI-1 and WNT-2, have been implicated in senescence (Kortlever et al., 2006; Ye et al., 2007). The expression of PAI-1 is under control of IL-6, as well as of C/EBPα, raising the interesting possibility that IL-6, C/EBP transcription factors, and the urokinase-dependent plasminogen activation system together constitute a stromal signaling network regulating cellular senescence.

An important role for the stroma is highlighted also by the property of senescent fibroblasts to secrete high levels of metalloproteinases, growth factors, and inflammatory cytokines (Campisi, 2005; this paper). In fact, this might reflect a counterproductive side effect of the organism's ability to limit the pool of incipient cancer cells by activating OIS. Indeed, senescent fibroblasts resemble those associated with cancer as well as wound healing (Campisi, 2005). Factors that are secreted by senescent fibroblasts can promote cell proliferation and tumorigenesis (Krtolica et al., 2001; this paper). A connection between senescence and inflammation is supported further by a recent hepatocellular carcinoma model, in which p53 reactivation led to senescence and subsequent elimination of the tumor mediated by the induction of a set of inflammatory cytokines (Xue et al., 2007). Interestingly, IL-6 levels increase also with aging (Hong et al., 2007). As our study implicates specific interleukins in cell-autonomous regulation of senescence, as well as in stimulation of proliferation, they arguably are endowed with the capacity to link senescence with aging, inflammation, and cancer.

EXPERIMENTAL PROCEDURES

Cell Culture, Viral Transduction, Cell Proliferation Assay, and Cell-Cycle Analysis

The human diploid fibroblast cell line Tig3 expressing the ecotropic receptor and hTERT ("Tig3(et)"), its *sh*-$p16^{INK4A}$-expressing derivative "Tig3(et)/16i," and human A375 melanoma cells were maintained in DMEM (GIBCO) supplemented with 9% fetal bovine serum (Greiner Bio-One), 2 mM glutamine, 100 units ml^{-1} penicillin, and 0.1 mg ml^{-1} streptomycin (all GIBCO). The human diploid fibroblast cell line IMR90 expressing the ecotropic receptor, shRNA for $p16^{INK4A}$, and hTERT ("IMR90(et)/16i") were maintained in MEM + Earle's salts (GIBCO) containing all supplements mentioned above and nonessential amino acids, 0.15% sodium bicarbonate, and 1 mM sodium pyruvate (all GIBCO). Normal human melanocytes were isolated, maintained, and lentivirally transduced as described (Michaloglou et al., 2005).

Retroviral transductions were performed with Phoenix cells as producers of viral supernatants as described (http://www.stanford.edu/group/nolan/retroviral_systems/phx.html). For cell proliferation assays, cells were typically infected with shRNA-encoding virus, briefly selected for successful proviral integration, and subsequently infected with $BRAF^{E600}$-encoding virus. Then, 4×10^5 cells were seeded into 6-well plates and fixed and stained 11–15 days postinfection with crystal violet or Coomassie Blue. BrdU analysis, STAT3-phosphorylation assay, and measurement of bioavailable IL-6 were performed as described in the Supplemental Experimental Procedures.

Plasmids

pMSCV-blast-$BRAF^{E600}$, pBABE-puro-$BRAF^{E600}$, pBABE-bleo-IL-6, pBABE-bleo-3′HA-IL-6, pLZRS-IRES-zeo-$Cdc42^{V12}$, and pBABE-puro-C/EBPβ (expressing the full-length cDNA with mutated [ATG → TTG] alternative start sites) were used for retroviral transduction. Sequences of shRNAs are described in the Supplemental Experimental Procedures.

Microarray Gene Expression Profiling

Total RNA from at least two independent experiments was isolated, purified, and amplified. Amplified RNA (aRNA) was subsequently labeled either with

(J) Protein levels of samples in (H), as determined by western blotting. β-actin serves as loading control.
(K) *IL6* transcript levels of samples in (H), as determined by qRT-PCR . Levels are represented relative to those found in control-infected cells, as mean + SD.

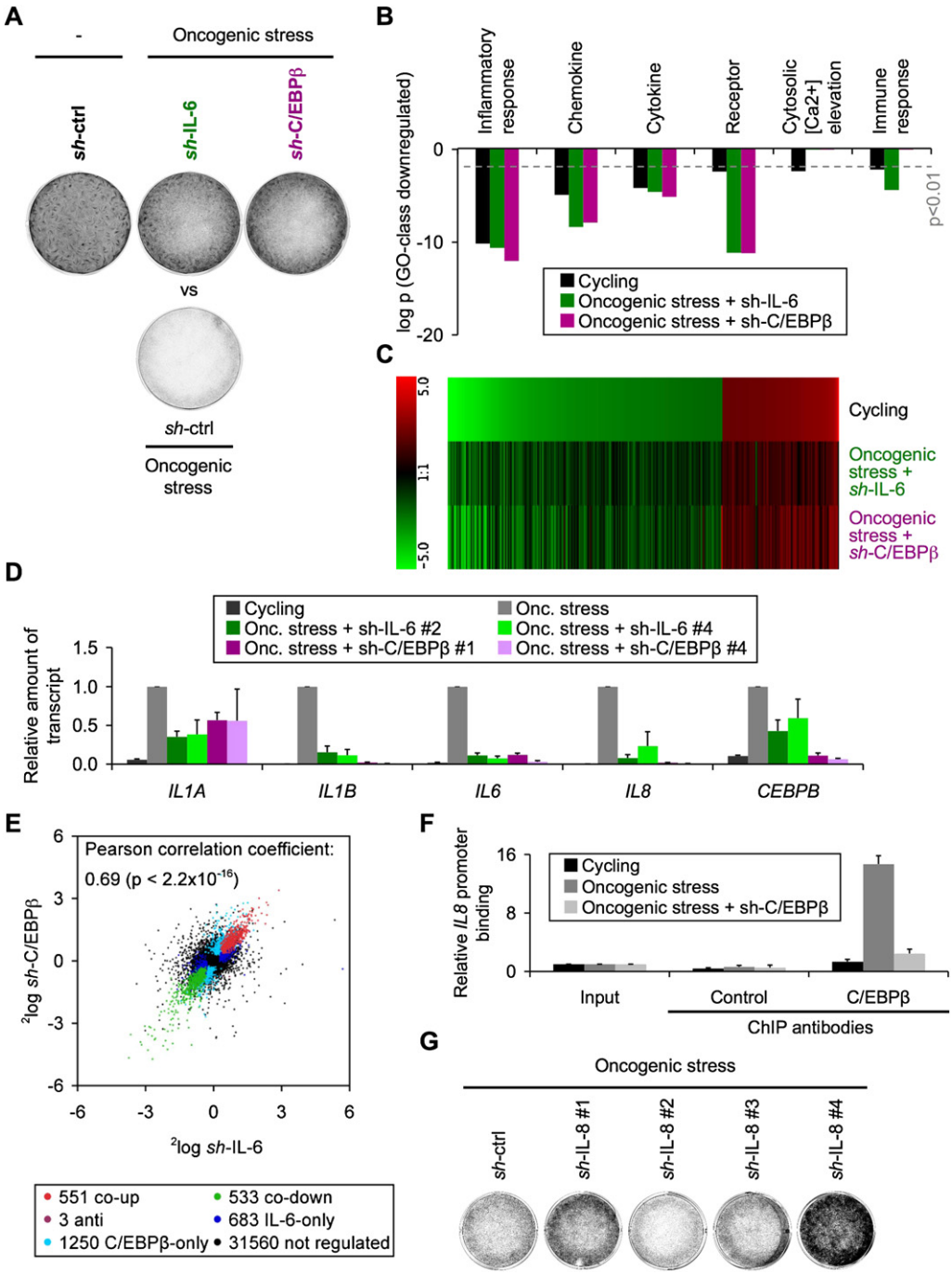

Figure 6. IL-6 Is a Central Regulator of an Inflammatory Network Mediating OIS

(A–E) Polyclonal Tig3(et)/16i cell lines expressing either *sh*-IL-6 or *sh*-C/EBPβ were exposed to oncogenic stress ($BRAF^{E600}$ retroviral transduction) and compared to cycling cells for their gene expression profiles. OIS cells serve as common reference.

(A) Cell proliferation assay and experimental outline.

(B) Microarray gene expression data were analyzed for regulation of GO classes. Six of 18 significantly ($p < 0.01$) downregulated classes are represented in the chart (the full panel of classes is represented in Figure S10).

(C) Heat map of M values of genes that are significantly ($-2 > M > 2$ and $p < 0.001$) regulated in cycling cells and cells that bypass OIS because of depletion of C/EBPβ or IL-6, with OIS as a general reference. Filters were applied on the complete gene expression data set, and genes were sorted according to M value in cycling cells.

(D) The levels of several interleukin transcripts were determined by qRT-PCR in cycling, OIS, and OIS bypass cells, as indicated. Data are represented as mean + SD.

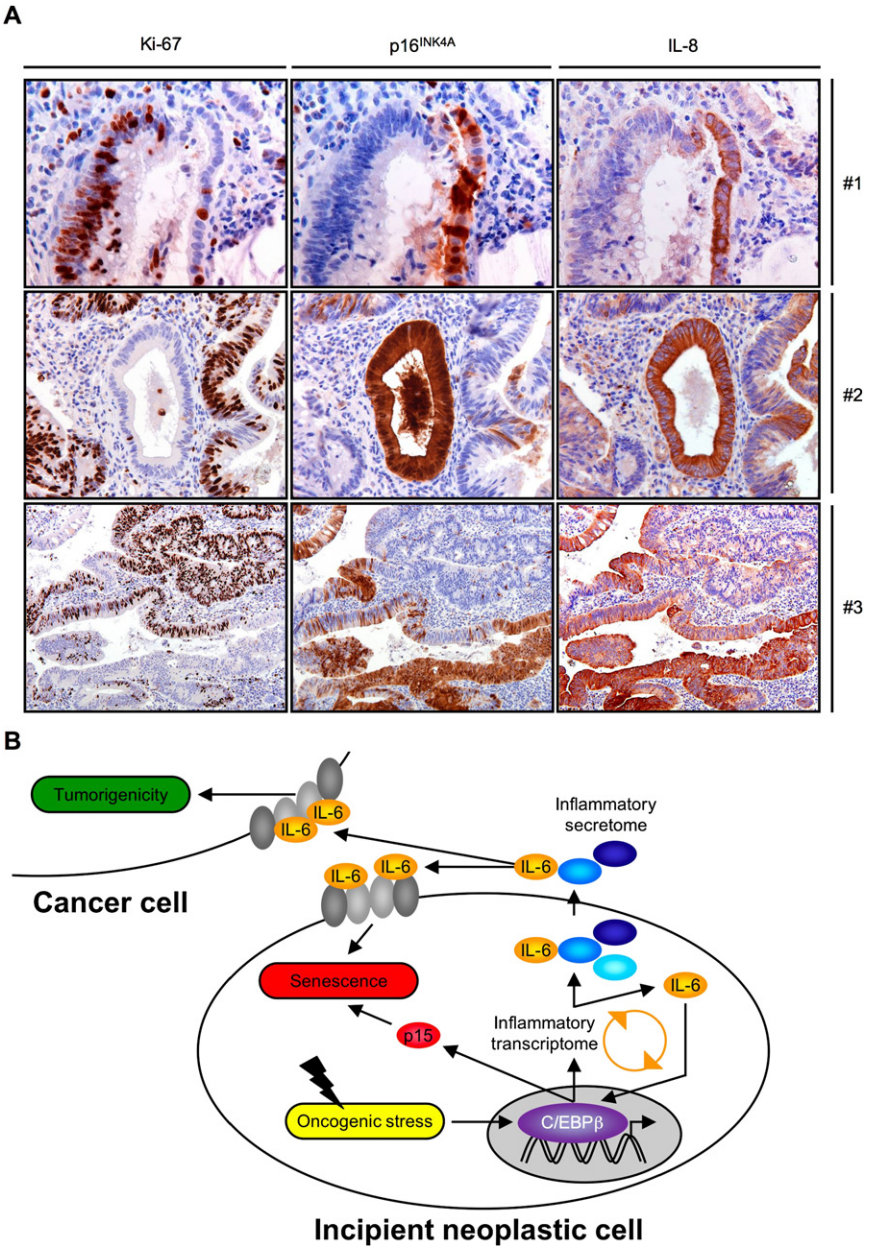

Figure 7. A Role for Interleukins In Vivo and a Model Reconciling the Antagonistic Functions of Interleukins in OIS and Cancer

(A) Consecutive 3-μm-thick paraffin sections of 20 FFPE human colon adenomas, ranging in size from 5 to 25 mm, were immunostained for IL-8, the proliferation marker Ki-67, and $p16^{INK4A}$. Three representative examples are shown (magnification upper two panels, 200×; lower panel, 100×). In addition to common overlapping immunopositivity for $p16^{INK4A}$ and IL-8 in arrested colon adenoma cells, some IL-8 positivity was detected in the distal part of normal colorectal crypts and in the surface epithelium but not in the basal parts of crypts (data not shown).

(B) Our results suggest a model in which a primary response to oncogenic stress corresponds to the establishment of a genetic inflammatory signature, in a C/EBPβ-dependent fashion. Effector genes include a set of interleukins, such as *IL6*, which operates in a positive feedback loop with C/EBPβ (orange circle), as well as *CDKN2B* (encoding $p15^{INK4B}$). Autocrine IL-6 signaling is essential for the cellular response to oncogenic stress; in its absence, cells fail to undergo OIS and continue proliferating. Although paracrine IL-6 signaling may also contribute to this, it is not essential. In a paracrine fashion, IL-6 can promote proliferation of susceptible (cancer) cells. Thus, depending on the context, specific interleukins elicit anti- (red) or proproliferative (green) effects, thereby affecting senescence and cancer.

Cy5 or Cy3. Labeled aRNA was hybridized to oligo arrays (Operon v3 library), and a dye-swap was performed for each experimental sample.

Gene ontology analysis is described in the Supplemental Experimental Procedures.

qRT-PCR

Total RNA was DNase treated with RQ1 RNase-Free DNase (Promega). Reverse transcription was performed with Superscript II first strand kit (Invitrogen). qRT-PCR was performed with the SYBR Green PCR Master Mix (Applied Biosystems) on an ABI PRISM 7700 Sequence Detection System. Primer sequences are described in the Supplemental Experimental Procedures.

Control primers were RPL13 and HPRT1. Except for C/EBPβ, all primer pairs span exon-exon barriers. Data are represented as mean + SD of three independent experiments.

Antibodies

Antibodies used for western blotting were against β-actin (AC-74; A5316; Sigma), BRAF (sc-5284; Santa Cruz), C/EBPβ (sc-150; Santa Cruz), IL-6 (AF-206-NA; R&D Systems), $p15^{INK4B}$ (sc-612; Santa Cruz), $p16^{INK4A}$ (JC8; MS-889; Neo-Markers), STAT3 (sc-482; Santa Cruz), and phospho-Tyr^{705}-STAT3 (3E2; #9138; Cell Signaling). The antibodies used for immunofluorescence were against trimethyl-Lys^{9}-histone H3 (07-442; Upstate) and IL-6 (AF-206-NA; R&D Systems).

Electrophoretic Mobility Shift Assay

A standard method was used for electrophoretic mobility shift assay (EMSA). Except for the consensus C/EBPβ binding site, probes correspond to the

(E) Two-sample correlation plot of oncogenically stressed cells depleted for either C/EBPβ or IL-6. The Pearson product-moment coefficient, reflecting the degree of linear relationship between two variables, was calculated as a measure of coregulation of the data sets; p value represents the probability that the correlation coefficient is 0 (null hypothesis).

(F) ChIP determining the in vivo binding of C/EBPβ to the *IL8* promoter upon exposure to oncogenic stress ($BRAF^{E600}$ retroviral infection). OIS Tig3(et)16i cells expressing *sh*-C/EBPβ were included as an extra control for the specificity of the C/EBPβ antibody. Relative *IL8* promoter binding was plotted as mean + SD.

(G) Cell proliferation assay of polyclonal Tig3(et)/16i HDF expressing independent shRNAs against IL-8 upon exposure to oncogenic stress (transduction with $BRAF^{E600}$-encoding retrovirus). Cells were fixed and stained 15 days after infection. (For concomitant quantification of *IL8* transcript levels, see Figure S11.)

nt −173 to nt −138 region within the human *IL6* promoter, spanning the CRE and C/EBPβ binding sites. To test specificity, probes were used with mutations in these binding sites. Probes and labeling technique are described in the Supplemental Experimental Procedures.

For competition binding assays, unlabeled probes were added to the reaction in 250× molar excess. For antibody treatment, nuclear extracts were preincubated with 2 μg C/EBPβ antibody (C-19; sc-150; Santa Cruz).

Chromatin Immunoprecipitation

ChIP was performed as described (Rowland et al., 2005) with the following modifications. Precleared chromatin was incubated with 2 μg control (TrkB: Santa Cruz sc-8316) or specific antibody (C/EBPβ: Cell Signaling #3087, Santa Cruz sc-150, or GeneTex MS-NFIL21-PX1); qPCR was performed with the Abi Prism 7700 Sequence Detection System and SYBR Green PCR Master Mix (Applied Biosystems). Primer sequences are described in the Supplemental Experimental Procedures. Relative promoter binding is represented as the ratio between the amount of specific and nonspecific amplified DNA fragments as mean + SD of three independent experiments.

Immunohistochemistry

Twenty formalin-fixed paraffin-embedded human colorectal tubular adenomas were immunostained for $p16^{INK4A}$ and proliferation marker Ki-67 (with MIB-1 antibody), as previously described (Michaloglou et al., 2005). Staining for IL-8 was performed with routine procedures; the antibody was from Bender MedSystems (BMS136; NAP II).

ACCESSION NUMBERS

The microarray data have been deposited in the ArrayExpress repository under accession numbers E-NCMF-12 and E-NCMF-13.

SUPPLEMENTAL DATA

Supplemental Data include Supplemental Experimental Procedures, Supplemental References, twelve figures, and two tables and can be found with this article online at http://www.cell.com/cgi/content/full/133/6/1019/DC1/.

ACKNOWLEDGMENTS

We thank P. Kortman and J. Zevenhoven for help with immunohistochemistry, M. Heimerikx for performing microarray experiments, E. de Wit, D. Sie, J. de Ronde, and R. Kerkhoven at the Microarray Facility for support analyzing expression data, E. de Groot for help with determining IL-6 levels in medium, B. Tolhuis for help with statistical analysis, A. Smith and B. Westerman for rsIL-6R-containing medium, M. Soengas for melanocytes, members of the Peeper laboratory for helpful discussions, J. Gil and J. Campisi for sharing unpublished data, and A. Sparmann, B. van Steensel, and A. Berns for critical reading of the manuscript. T.K., L.C.W.V., C.M., S.D., and D.S.P. have been supported by Netherlands Organisation for Scientific Research Vidi and Vici grants and by grants from the Dutch Cancer Society (KWF), C.J.D. by a European FP6 program, and R.v.D. by a KWF fellowship for medical specialists; D.S.P. received support also from the EMBO Young Investigator program.

Received: September 21, 2007
Revised: December 28, 2007
Accepted: March 31, 2008
Published: June 12, 2008

REFERENCES

Acosta, J.C., O'Loghlen, A., Banito, A., Guijarro, M.V., Augert, A., Raguz, S., Fumagalli, M., Da Costa, M., Brown, C., Popov, N., et al. (2008). Chemokine Signaling via the CXCR2 Receptor Reinforces Senescence. Cell *133*, this issue, 1006–1018.

Adams, P.D. (2007). Remodeling of chromatin structure in senescent cells and its potential impact on tumor suppression and aging. Gene *397*, 84–93.

Ancrile, B., Lim, K.H., and Counter, C.M. (2007). Oncogenic Ras-induced secretion of IL6 is required for tumorigenesis. Genes Dev. *21*, 1714–1719.

Bartkova, J., Rezaei, N., Liontos, M., Karakaidos, P., Kletsas, D., Issaeva, N., Vassiliou, L.V., Kolettas, E., Niforou, K., Zoumpourlis, V.C., et al. (2006). Oncogene-induced senescence is part of the tumorigenesis barrier imposed by DNA damage checkpoints. Nature *444*, 633–637.

Beausejour, C.M., Krtolica, A., Galimi, F., Narita, M., Lowe, S.W., Yaswen, P., and Campisi, J. (2003). Reversal of human cellular senescence: Roles of the p53 and p16 pathways. EMBO J. *22*, 4212–4222.

Berns, K., Hijmans, E.M., Mullenders, J., Brummelkamp, T.R., Velds, A., Heimerikx, M., Kerkhoven, R.M., Madiredjo, M., Nijkamp, W., Weigelt, B., et al. (2004). A large-scale RNAi screen in human cells identifies new components of the p53 pathway. Nature *428*, 431–437.

Braig, M., Lee, S., Loddenkemper, C., Rudolph, C., Peters, A.H., Schlegelberger, B., Stein, H., Dorken, B., Jenuwein, T., and Schmitt, C.A. (2005). Oncogene-induced senescence as an initial barrier in lymphoma development. Nature *436*, 660–665.

Brakenhoff, J.P., de Hon, F.D., Fontaine, V., ten Boekel, E., Schooltink, H., Rose-John, S., Heinrich, P.C., Content, J., and Aarden, L.A. (1994). Development of a human interleukin-6 receptor antagonist. J. Biol. Chem. *269*, 86–93.

Campisi, J. (2005). Senescent cells, tumor suppression, and organismal aging: Good citizens, bad neighbors. Cell *120*, 513–522.

Chen, Z., Trotman, L.C., Shaffer, D., Lin, H.K., Dotan, Z.A., Niki, M., Koutcher, J.A., Scher, H.I., Ludwig, T., Gerald, W., et al. (2005). Crucial role of p53-dependent cellular senescence in suppression of Pten-deficient tumorigenesis. Nature *436*, 725–730.

Collado, M., Gil, J., Efeyan, A., Guerra, C., Schuhmacher, A.J., Barradas, M., Benguria, A., Zaballos, A., Flores, J.M., Barbacid, M., et al. (2005). Tumour biology: Senescence in premalignant tumours. Nature *436*, 642.

Courtois-Cox, S., Genther Williams, S.M., Reczek, E.E., Johnson, B.W., McGillicuddy, L.T., Johannessen, C.M., Hollstein, P.E., MacCollin, M., and Cichowski, K. (2006). A negative feedback signaling network underlies oncogene-induced senescence. Cancer Cell *10*, 459–472.

Dai, C.Y., Furth, E.E., Mick, R., Koh, J., Takayama, T., Niitsu, Y., and Enders, G.H. (2000). p16(INK4a) expression begins early in human colon neoplasia and correlates inversely with markers of cell proliferation. Gastroenterology *119*, 929–942.

Dankort, D., Filenova, E., Collado, M., Serrano, M., Jones, K., and McMahon, M. (2007). A new mouse model to explore the initiation, progression, and therapy of BRAFV600E-induced lung tumors. Genes Dev. *21*, 379–384.

Davies, H., Bignell, G.R., Cox, C., Stephens, P., Edkins, S., Clegg, S., Teague, J., Woffendin, H., Garnett, M.J., Bottomley, W., et al. (2002). Mutations of the BRAF gene in human cancer. Nature *417*, 949–954.

Denoyelle, C., Abou-Rjaily, G., Bezrookove, V., Verhaegen, M., Johnson, T.M., Fullen, D.R., Pointer, J.N., Gruber, S.B., Su, L.D., Nikiforov, M.A., et al. (2006). Anti-oncogenic role of the endoplasmic reticulum differentially activated by mutations in the MAPK pathway. Nat. Cell Biol. *8*, 1053–1063.

Di Micco, R., Fumagalli, M., Cicalese, A., Piccinin, S., Gasparini, P., Luise, C., Schurra, C., Garre, M., Nuciforo, P.G., Bensimon, A., et al. (2006). Oncogene-induced senescence is a DNA damage response triggered by DNA hyper-replication. Nature *444*, 638–642.

Dimri, G.P., Lee, X., Basile, G., Acosta, M., Scott, G., Roskelley, C., Medrano, E.E., Linskens, M., Rubelj, I., Pereira-Smith, O., et al. (1995). A biomarker that identifies senescent human cells in culture and in aging skin in vivo. Proc. Natl. Acad. Sci. USA *92*, 9363–9367.

Dirac, A.M., and Bernards, R. (2003). Reversal of senescence in mouse fibroblasts through lentiviral suppression of p53. J. Biol. Chem. *278*, 11731–11734.

Finkel, T., Serrano, M., and Blasco, M.A. (2007). The common biology of cancer and ageing. Nature *448*, 767–774.

Garnett, M.J., and Marais, R. (2004). Guilty as charged: B-RAF is a human oncogene. Cancer Cell *6*, 313–319.

Gomis, R.R., Alarcon, C., Nadal, C., Van Poznak, C., and Massague, J. (2006). C/EBPbeta at the core of the TGFbeta cytostatic response and its evasion in metastatic breast cancer cells. Cancer Cell *10*, 203–214.

Gray-Schopfer, V.C., Cheong, S.C., Chong, H., Chow, J., Moss, T., Abdel-Malek, Z.A., Marais, R., Wynford-Thomas, D., and Bennett, D.C. (2006). Cellular senescence in naevi and immortalisation in melanoma: A role for p16? Br. J. Cancer *95*, 496–505.

Ha, L., Ichikawa, T., Anver, M., Dickins, R., Lowe, S., Sharpless, N.E., Krimpenfort, P., Depinho, R.A., Bennett, D.C., Sviderskaya, E.V., et al. (2007). ARF functions as a melanoma tumor suppressor by inducing p53-independent senescence. Proc. Natl. Acad. Sci. USA *104*, 10968–10973.

Hirano, T., and Kishimoto, T. (1989). Interleukin-6: Possible implications in human diseases. Ric. Clin. Lab. *19*, 1–10.

Hodge, D.R., Xiao, W., Clausen, P.A., Heidecker, G., Szyf, M., and Farrar, W.L. (2001). Interleukin-6 regulation of the human DNA methyltransferase (HDNMT) gene in human erythroleukemia cells. J. Biol. Chem. *276*, 39508–39511.

Hong, D.S., Angelo, L.S., and Kurzrock, R. (2007). Interleukin-6 and its receptor in cancer: Implications for Translational Therapeutics. Cancer *110*, 1911–1928.

Kalai, M., Montero-Julian, F.A., Brakenhoff, J.P., Fontaine, V., De Wit, L., Wollmer, A., Brailly, H., Content, J., and Grotzinger, J. (1997). Analysis of the mechanism of action of anti-human interleukin-6 and anti-human interleukin-6 receptor-neutralising monoclonal antibodies. Eur. J. Biochem. *249*, 690–700.

Kortlever, R.M., Higgins, P.J., and Bernards, R. (2006). Plasminogen activator inhibitor-1 is a critical downstream target of p53 in the induction of replicative senescence. Nat. Cell Biol. *8*, 877–884.

Krimpenfort, P., Ijpenberg, A., Song, J.Y., van der Valk, M., Nawijn, M., Zevenhoven, J., and Berns, A. (2007). p15Ink4b is a critical tumour suppressor in the absence of p16Ink4a. Nature *448*, 943–946.

Krtolica, A., Parrinello, S., Lockett, S., Desprez, P.Y., and Campisi, J. (2001). Senescent fibroblasts promote epithelial cell growth and tumorigenesis: A link between cancer and aging. Proc. Natl. Acad. Sci. USA *98*, 12072–12077.

Lloyd, A.C., Obermuller, F., Staddon, S., Barth, C.F., McMahon, M., and Land, H. (1997). Cooperating oncogenes converge to regulate cyclin/cdk complexes. Genes Dev. *11*, 663–677.

Lowe, S.W., Cepero, E., and Evan, G. (2004). Intrinsic tumour suppression. Nature *432*, 307–315.

Lu, C., and Kerbel, R.S. (1993). Interleukin-6 undergoes transition from paracrine growth inhibitor to autocrine stimulator during human melanoma progression. J. Cell Biol. *120*, 1281–1288.

Mallette, F.A., Gaumont-Leclerc, M.F., and Ferbeyre, G. (2007). The DNA damage signaling pathway is a critical mediator of oncogene-induced senescence. Genes Dev. *21*, 43–48.

Mason, D.X., Jackson, T.J., and Lin, A.W. (2004). Molecular signature of oncogenic ras-induced senescence. Oncogene *23*, 9238–9246.

Michaloglou, C., Vredeveld, L.C., Soengas, M.S., Denoyelle, C., Kuilman, T., van der Horst, C.M., Majoor, D.M., Shay, J.W., Mooi, W.J., and Peeper, D.S. (2005). BRAFE600-associated senescence-like cell cycle arrest of human naevi. Nature *436*, 720–724.

Mooi, W.J., and Peeper, D.S. (2006). Oncogene-induced cell senescence–halting on the road to cancer. N. Engl. J. Med. *355*, 1037–1046.

Narita, M., Nunez, S., Heard, E., Narita, M., Lin, A.W., Hearn, S.A., Spector, D.L., Hannon, G.J., and Lowe, S.W. (2003). Rb-mediated heterochromatin formation and silencing of E2F target genes during cellular senescence. Cell *113*, 703–716.

Nicke, B., Bastien, J., Khanna, S.J., Warne, P.H., Cowling, V., Cook, S.J., Peters, G., Delpuech, O., Schulze, A., Berns, K., et al. (2005). Involvement of MINK, a Ste20 family kinase, in Ras oncogene-induced growth arrest in human ovarian surface epithelial cells. Mol. Cell *20*, 673–685.

Peeper, D.S., Shvarts, A., Brummelkamp, T., Douma, S., Koh, E.Y., Daley, G.Q., and Bernards, R. (2002). A functional screen identifies hDRIL1 as an oncogene that rescues RAS-induced senescence. Nat. Cell Biol. *4*, 148–153.

Ramji, D.P., and Foka, P. (2002). CCAAT/enhancer-binding proteins: Structure, function and regulation. Biochem. J. *365*, 561–575.

Rowland, B.D., Bernards, R., and Peeper, D.S. (2005). The KLF4 tumour suppressor is a transcriptional repressor of p53 that acts as a context-dependent oncogene. Nat. Cell Biol. *7*, 1074–1082.

Sage, J., Miller, A.L., Perez-Mancera, P.A., Wysocki, J.M., and Jacks, T. (2003). Acute mutation of retinoblastoma gene function is sufficient for cell cycle re-entry. Nature *424*, 223–228.

Schnabl, B., Purbeck, C.A., Choi, Y.H., Hagedorn, C.H., and Brenner, D. (2003). Replicative senescence of activated human hepatic stellate cells is accompanied by a pronounced inflammatory but less fibrogenic phenotype. Hepatology *37*, 653–664.

Sebastian, T., Malik, R., Thomas, S., Sage, J., and Johnson, P.F. (2005). C/EBPbeta cooperates with RB:E2F to implement Ras(V12)-induced cellular senescence. EMBO J. *24*, 3301–3312.

Shay, J.W., and Wright, W.E. (2005). Senescence and immortalization: Role of telomeres and telomerase. Carcinogenesis *26*, 867–874.

Sherr, C.J. (2004). Principles of tumor suppression. Cell *116*, 235–246.

Sparmann, A., and Bar-Sagi, D. (2004). Ras-induced interleukin-8 expression plays a critical role in tumor growth and angiogenesis. Cancer Cell *6*, 447–458.

Tremain, R., Marko, M., Kinnimulki, V., Ueno, H., Bottinger, E., and Glick, A. (2000). Defects in TGF-beta signaling overcome senescence of mouse keratinocytes expressing v-Ha-ras. Oncogene *19*, 1698–1709.

Xue, W., Zender, L., Miething, C., Dickins, R.A., Hernando, E., Krizhanovsky, V., Cordon-Cardo, C., and Lowe, S.W. (2007). Senescence and tumour clearance is triggered by p53 restoration in murine liver carcinomas. Nature *445*, 656–660.

Ye, X., Zerlanko, B., Kennedy, A., Banumathy, G., Zhang, R., and Adams, P.D. (2007). Downregulation of Wnt signaling is a trigger for formation of facultative heterochromatin and onset of cell senescence in primary human cells. Mol. Cell *27*, 183–196.